The Structural Basis of Cholesterol Accessibility in Membranes

Brett N. Olsen,[†] Agata A. Bielska,[†] Tiffany Lee,[†] Michael D. Daily,[‡] Douglas F. Covey,[§] Paul H. Schlesinger,[¶] Nathan A. Baker,[‡] and Daniel S. Ory[†*]

[†]Diabetic Cardiovascular Disease Center, Washington University School of Medicine, St. Louis, Missouri; [‡]Knowledge Discovery and Informatics, Pacific Northwest National Laboratory, Richland, Washington; [§]Department of Developmental Biology and [¶]Department of Cell Biology and Physiology, Washington University School of Medicine, St. Louis, Missouri

ABSTRACT Although the majority of free cellular cholesterol is present in the plasma membrane, cholesterol homeostasis is principally regulated through sterol-sensing proteins that reside in the cholesterol-poor endoplasmic reticulum (ER). In response to acute cholesterol loading or depletion, there is rapid equilibration between the ER and plasma membrane cholesterol pools, suggesting a biophysical model in which the availability of plasma membrane cholesterol for trafficking to internal membranes modulates ER membrane behavior. Previous studies have predominantly examined cholesterol availability in terms of binding to extramembrane acceptors, but have provided limited insight into the structural changes underlying cholesterol activation. In this study, we use both molecular dynamics simulations and experimental membrane systems to examine the behavior of cholesterol in membrane bilayers. We find that cholesterol depth within the bilayer provides a reasonable structural metric for cholesterol availability and that this is correlated with cholesterol-acceptor binding. Further, the distribution of cholesterol availability in our simulations is continuous rather than divided into distinct available and unavailable pools. This data provide support for a revised cholesterol activation model in which activation is driven not by saturation of membrane-cholesterol interactions but rather by bulk membrane remodeling that reduces membrane-cholesterol affinity.

INTRODUCTION

Cholesterol is the most abundant sterol present in mammalian cells, and is essential for cellular function and viability (1–3). Cholesterol primarily serves as a structural component of cellular membranes, where it contributes to the physical behavior of membranes by modulating membrane permeability, fluidity, and phase (4–9). The importance of cholesterol to membrane function is underscored by the diverse regulatory pathways that maintain cellular cholesterol levels within a narrow range. Although the majority of free cellular cholesterol is present in the plasma membrane, homeostatic responses to acute changes in cellular cholesterol content principally occur in the endoplasmic reticulum (ER) (1–3,10–14). These intracellular regulatory pathways respond rapidly to changes in plasma membrane cholesterol levels (15,16).

To address how the ER regulatory machinery senses changes in plasma membrane cholesterol levels, a biophysical model for cholesterol behavior in cellular membranes has emerged (15–18). This model, termed the active cholesterol hypothesis, posits that under cholesterol-replete conditions, plasma membrane cholesterol is unavailable for trafficking to the ER because it is tightly complexed with phospholipids. Accordingly, above a threshold concentration where cholesterol-binding sites become saturated, the excess cholesterol becomes available for transfer to the ER to trigger regulatory responses. This movement of cholesterol from unavailable to available states is termed cholesterol activation, and is likely related to changes in the thermodynamic activity of cholesterol molecules within the bilayer.

In a series of elegant studies, Lange, Steck, and co-workers (15,17) have demonstrated that changes in sterol homeostatic responses occur rapidly over very narrow cholesterol concentrations, centered around the physiological cholesterol regulatory setpoint. Direct measurements of cholesterol activation made using diverse cholesterol-binding molecules including cholesterol oxidase, β-cyclodextrin, and perfringolysin O (PFO) show sharp increases in cholesterol availability to these acceptors above the physiological threshold (15,19–21). Activation of intracellular regulatory pathways can be triggered not only by excess cholesterol but also by the addition of small-molecule amphiphiles known to increase cholesterol accessibility in model systems (15,16). Further, experiments performed on cholesterol-enriched or -depleted cells show that activation of cholesterol in liposomes reconstituted from extracted ER lipids occurs at the same concentration threshold as cholesterol-mediated suppression of SREBP proteolysis (19). This data suggest that cholesterol accessibility regulates trafficking of plasma membrane cholesterol to intracellular compartments as well as directly controlling cholesterol homeostasis through modulation of the ER sterol-sensing proteins.

Cholesterol activation is protein-independent, because activation thresholds are observed in defined artificial liposomes containing only lipids (19,20). The observed thresholds are highly dependent on membrane composition, with saturated lipids having higher activation thresholds than unsaturated lipids (19). In cells, low concentrations

Submitted February 21, 2013, and accepted for publication August 30, 2013.

*Correspondence: dory@dom.wustl.edu

Editor: Scott Feller.

© 2013 by the Biophysical Society

0006-3495/13/10/1838/10 $2.00

http://dx.doi.org/10.1016/j.bpj.2013.08.042

of side-chain oxysterols trigger cholesterol esterification, which is indicative of cholesterol trafficking from the plasma membrane to the ER and consistent with our previous work showing that oxysterols promote cholesterol activation in model membranes (14,22,23). Moreover, various small molecule amphiphiles have also been found to lower the cholesterol activation threshold when partitioned into membranes as well as triggering intracellular responses to elevated cholesterol (15,16,24).

These findings suggest that the mechanisms of cholesterol activation are rooted in the fundamental interactions between cholesterol and the membrane environment and are central to regulation of cholesterol homeostasis. As of this writing, cholesterol activation is experimentally determined by directly measuring the availability of cholesterol to an extramembrane acceptor or probe. To gain insight into the structural basis of cholesterol activation, we have performed molecular dynamics simulations of simple membrane models. These simulations, which provide atomic-scale resolution of small membrane systems, allow us to identify changes in general membrane properties as well as conformation and structure of individual cholesterol molecules in membranes of varying cholesterol concentrations. We have further complemented the structural detail provided by molecular dynamics simulations by obtaining experimental measures of cholesterol availability in membranes of identical composition. Taken together, these approaches allow us to identify changes in membrane structure and cholesterol behavior that are associated with cholesterol activation and provide what we believe to be new insights into the biophysical mechanisms that permit rapid nontranscriptional responses to acute cholesterol loads.

MATERIALS AND METHODS

Molecular dynamics simulations

Cholesterol and POPC (1-palmitoyl-2-oleoyl-phosphatidylcholine) parameters and charges were used as described previously (23,25). DOPC (dioleoylphosphatidylcholine) lipids were simulated using the united atom parameters of Berger et al. (26). We prepared membrane systems containing 256 POPC or DOPC molecules and an additional 0, 16, 28, 56, 84, 112, 148, 178, 210, or 278 cholesterol molecules, corresponding to mol % cholesterol of 0, 6, 10, 18, 25, 30, 37, 41, 45, and 51%. The 0, 18, and 30% cholesterol in POPC simulations have already been described in Olsen et al. (23,25). The 0, 18, and 30% cholesterol in DOPC simulations were prepared similarly and these concentrations were used as starting points for preparation of the other simulations.

Systems were prepared in the following manner. Subsections of the 0% simulations were taken containing $(256 + X)/4$ total phospholipids (rounded up), where X is the number of cholesterol molecules required in the final structure. The X phospholipids were replaced with cholesterol structures sampled from the 30% simulations, and any steric clashes resolved in a similar manner as described by Kandt et al. (27) for membrane protein insertion. To start, the membrane was stretched laterally threefold by scaling the positions of each lipid in the bilayer plane. This was followed by a series of energy minimization and small lateral compression steps until returned to the original size. These smaller bilayers were replicated 2×2 in the bilayer plane, and any excess cholesterol molecules (due to rounding) were removed. These structures were solvated with SPC water molecules (28) and K^+ and Cl^- ions to ~55 waters per lipid (both phospholipid and cholesterol) and a KCl concentration of 115mM. These structures were then warmed to 300 K in 50 K increments, simulated for 50 ps at each temperature before being used as starting points for the production simulations.

All molecular dynamics simulations were performed using GROMACS, Vers. 3.3.1, 4.0, or 4.5 (29,30). All simulations followed the same molecular dynamics protocol as described in our previous work (23,25). Production simulations were run for 400 ns of total simulation time. Based on examination of membrane projected area and system energy drift, we chose to discard the first 200 ns of each simulation as equilibration time, leaving 200 ns of steady-state simulation time for analysis of each membrane composition. We analyzed system snapshots every 100 ps, for a total of 2001 frames per system. Statistical comparisons between simulations were done treating individual lipids independently with an estimated 5 ns relaxation time between independent samples of individual lipid or general membrane properties, based on autocorrelation times of membrane-projected areas.

Simulation analysis methods

Solvent-accessible surface area

Solvent-accessible surface area (SASA) calculations were performed as described in our previous work (23,25). Briefly, solvent was removed from system structures and the structure replicated in the bilayer plane. SASAs of individual lipid atoms were calculated from these structures using the acc submodule of the software APBS, Ver. 1.0.0 (31), using a 1.4 Å radius solvent probe. Lipids in the replicated bilayer images were discarded, and the contributions from each lipid's atom in the central image were summed to obtain a molecular exposed surface area for each lipid.

Phospholipid order parameters

Phospholipid order parameters were calculated as described in our previous work (23,25). Briefly, lipid-tail order is characterized by the order parameter tensor for each tail atom i (32–34):

$$S_{\alpha\beta}(i) = \frac{1}{2}\langle 3\cos\theta_\alpha(i)\cos\theta_\beta(i) - \delta_{\alpha\beta}\rangle, \qquad (1)$$

where $\alpha,\beta = x, y, z$ and $\theta_\alpha(i)$ denote the angle between the z axis and the αth axis of the ith atom. For our united atom systems, we estimate $\theta_z(i)$ as the angle between the vector pointing from the $(i + 1)$th atom to the $(i - 1)$th atom and the z axis. We report

$$|S_{CD}(i)| = \left|-\frac{1}{2}S_{zz}\right|$$

as a good measure of the extension of the lipid chains.

Phospholipid interdigitation

Lipid interdigitation was calculated from lipid mass density profiles. Mass densities were calculated separately for phospholipids in the upper and lower leaflets of each bilayer in 0.1 Å windows along the bilayer normal axis from systems centered along the bilayer normal axis. Interdigitation was then defined as the fractional overlap between these densities:

$$I = \frac{2\int_{-L/2}^{L/2}\min\left(\rho_{\text{lower}}(z),\rho_{\text{upper}}(z)\right)dz}{\int_{-L/2}^{L/2}\rho_{\text{lower}}(z) + \int_{-L/2}^{L/2}\rho_{\text{upper}}(z)}. \qquad (2)$$

Lipid neighbors

Lipid neighbor relationships were analyzed by initially isolating the upper and lower leaflets of the membrane and then calculating the center of position of each lipid in the plane of the bilayer. A periodic two-dimensional Delaunay triangulation on the lipid positions in each leaflet was performed to identify lipid-lipid neighbors on the resulting connected undirected graph of lipids.

Water interface, cholesterol depth, and membrane thickness

Water interface positions were calculated from water mass density profiles calculated in 0.1 Å windows along the bilayer normal axis from systems centered along the bilayer normal axis. To begin, the raw density profiles were smoothed with a 0.5 Å pointed window smoothing algorithm. Water interface positions were then defined as the points at which the smoothed water density reached half of its bulk density. Cholesterol depth was defined for individual cholesterol molecules as the relative distance along the bilayer normal axis between the cholesterol hydroxyl oxygen atom and the nearest water interface, with negative values denoting cholesterols closer to the bilayer center than the water interface. Membrane thickness was calculated as the distance between the upper and lower leaflet interfaces. Membrane volume was defined as the product of the membrane thickness and the projected area of the system box in the plane of the bilayer.

Protein-liposome binding experiments

The His^6-PFO (C459A) expression construct in the pRSETB vector (Invitrogen, Carlsbad, CA) was kindly provided by A. Heuck (University of Massachusetts, Amherst, MA) (20), and was transformed into BL21-CodonPlus(DE3)-RIPL *Escherichia coli* competent cells (Stratagene, La Jolla, CA). Protein expression and purification was performed according to manufacturer instructions and as described in Flanagan et al. (20). The pooled fractions containing PFO were concentrated using an Amicon Ultra 10-kDa cutoff centrifugal filter (Millipore, Billerica, MA). The PFO concentration was adjusted so that, following the addition of 10% (v/v) glycerol, the final concentration was 4–8 mg/mL. PFO was aliquoted, flash-frozen in liquid nitrogen, and stored at −80°C.

Phospholipids and cholesterol were obtained from Steraloids (Newport, RI). Liposomes were synthesized and PFO binding experiments were performed as described in Sokolov and Radhakrishnan (19) and Pan et al. (35). Briefly, PFO binding was assessed in 96-well plates (Corning, Corning, NY) with 200 μL reaction mixtures containing 4 μM PFO and 800 μM liposomes in buffer (150 mM NaCl, 50 mM Tris-HCl, pH 7.4). After incubation at 37°C for 1 h, tryptophan fluorescence was measured (excitation wavelength 290 nm; emission wavelength 340 nm; band-pass 5 nm) using an infinite 200 microplate reader (Tecan Group, Männedorf, Switzerland). Fluorescence measurements are displayed as F/F_0, where F is the measured fluorescence, and F_0 the fluorescence of unbound PFO (as measured in liposomes with either 0 or 20 mol % cholesterol in DOPC). Increased fluorescence is indicative of PFO binding.

RESULTS

Membrane condensation and relaxation

Cholesterol is well known to induce the condensation of membranes and neighboring phospholipids (6,7,36–40). The SASA of each phospholipid was calculated as a proxy for lipid condensation, as shown in Fig. 1 *A* (23). We find that from 0 to 25 mol % cholesterol, the exposed surface area of both POPC and DOPC phospholipids is significantly reduced, corresponding to condensation of the phospholipids and tighter lipid packing. POPC, which has one saturated and one unsaturated acyl chain, shows a decrease in mean surface area of 11.0 $Å^2$, whereas DOPC, with two unsaturated acyl chains, only shows a decrease of 6.8 $Å^2$, consistent with experimental data demonstrating that cholesterol is better at condensing saturated than unsaturated lipids (6,7). From 25 to 52 mol % cholesterol, we find a reversal of these effects, observing large increases in phospholipid surface area of 37.9 $Å^2$ for POPC and 35.1 $Å^2$ for DOPC phospholipids. However, phospholipid SASA is an imperfect proxy for lipid condensation: it measures the exposed surface area of the lipid, which can be increased by either looser packing of the lipids providing more lateral area per lipid, or by changes in headgroup conformation that allow more exposed surface area for a given lateral area. Thus, the large increases in surface area observed at high cholesterol concentrations could be due to a reduction in membrane condensation, or to an increase in exposed headgroup conformations, or a combination of both.

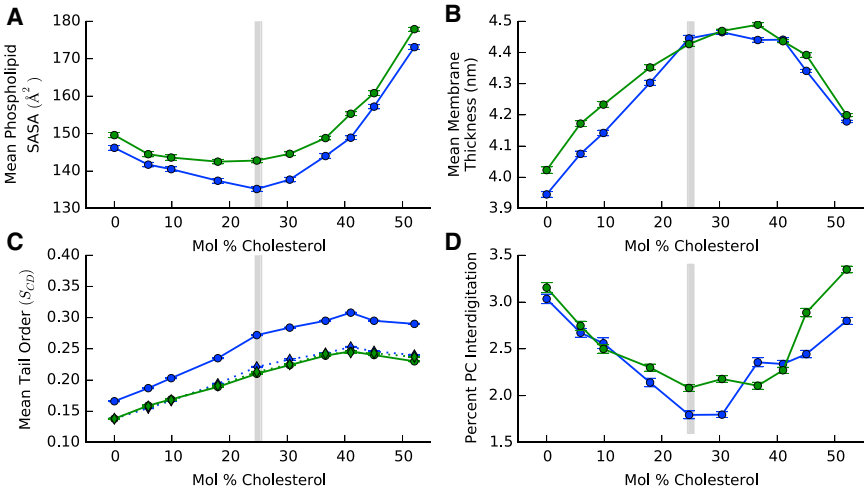

FIGURE 1 Various metrics of lipid condensation in POPC (*blue*) or DOPC (*green*) phospholipid membranes of varying cholesterol concentrations. Error bars show standard deviations of the mean, calculated using a bootstrap method. (*Gray-shaded zone*) Estimated division between condensing and relaxing regimes, at 25 mol % cholesterol. (*A*) Mean solvent-accessible surface area of single phospholipids. (*B*) Mean membrane thickness. (*C*) Mean tail-order parameters of the sn-1 (*solid*) and sn-2 (*dotted*) phospholipid tails. (*D*) Phospholipid interdigitation, measured as percentage overlap between phospholipid mass densities in each leaflet.

To further understand the observed membrane behavior at high cholesterol concentrations, we calculated the thickness of the simulated membranes. Because our simulated membranes are volume-incompressible and membrane volume is a linear combination of lipid volumes (see Fig. S1 in the Supporting Material), changes in membrane thickness are directly proportional to lateral packing. From 0 to 25 mol % cholesterol, both DOPC and POPC membranes increase in thickness (Fig. 1 *B*). This increase corresponds to tighter lateral packing, which is indicative of membrane condensation. Above 25 mol % cholesterol, membrane thickness plateaus and then decreases, indicating looser lateral packing of lipids and a partial decondensation or relaxation of the membrane structure. This partial thinning at very high cholesterol concentrations is consistent with other simulations of DOPC membranes (37).

Phospholipid-tail order measures the alignment of lipid-tail atoms, with larger values denoting a chain that is more aligned with the bilayer normal axis (7,23,25,36–40). Higher tail-order parameters indicate straighter acyl chains that pack more efficiently, and are strongly associated with membrane condensation. Mean order parameters across all carbons in the sn-1 and sn-2 chains of both DOPC and POPC lipids are shown in Fig. 1 *C*. In the 0–25 mol % range, we see strong ordering of the lipid tails, which improves lipid packing and is consistent with other measures of membrane condensation. At higher concentrations, however, we do not see a reversal of this ordering, instead finding that tail order increases slightly before stabilizing at higher, ordered values. This indicates that the membrane changes we observe at high cholesterol concentrations—partial membrane thinning and increased lipid exposure—are not driven by disordering of the lipid tails.

The decrease in membrane thickness at high cholesterol concentrations could be derived from two different physical causes:

1. The phospholipids could decrease their individual thickness by folding up or tilting their acyl chains so as to take up less space along the bilayer normal axis.
2. The phospholipids could interdigitate their acyl chains so that phospholipids in different leaflets would overlap their chains and decrease the total thickness of the membrane, though not the thickness of each individual lipid.

Any change in acyl-chain behavior that would decrease its individual thickness would be observed as a decrease in lipid order parameters, indicating that this is not the root cause of the membrane thinning.

To identify whether increased lipid interdigitation was responsible for membrane thinning, we measured the interdigitation of phospholipid tails (Fig. 1 *D*). From 0 to 25 mol % cholesterol, interdigitation is reduced significantly in both POPC and DOPC bilayers, indicating that membrane condensation both improves lipid packing and reduces interactions between leaflets. At higher concentrations, however, this reduction in interdigitation is completely reversed. Thus, whereas the increase in thickness at lower concentrations is driven by acyl-chain ordering, the decrease at higher concentrations is caused by an increase in interdigitation between the ordered lipid tails.

In general, we observe two different kinds of overall membrane behavior as the cholesterol concentration increases. At low concentrations, up to a threshold of roughly 20–30 mol %, additional cholesterol condenses the membrane, improving lipid packing, ordering the acyl chains of the lipids, thickening the membrane, and reducing membrane interdigitation. Above this threshold, we see no further membrane condensation, but instead observe a set of changes we term as a relaxation of the membrane to distinguish it from simply a reversal of condensation. This membrane relaxation is marked by a decrease in thickness and increased lipid exposure, but it is not simply a reversal of the membrane condensation, because these changes are not caused by lipid disordering but instead by increased lipid interdigitation.

Cholesterol activation

PFO is a cholesterol-dependent cytolysin that binds specifically to membranes that contain available cholesterol (19,20,41). Because insertion of PFO into membranes is dependent on cholesterol and shows a threshold response, PFO is able to serve as a sensor of available cholesterol. PFO binding to phospholipid/cholesterol liposomes was used to measure cholesterol activation in liposomes containing varying concentrations of cholesterol (Fig. 2 *A*). Sigmoidal curves were fitted to the binding data and activation thresholds estimated from the fitted curves (shown in the figure as *shaded bars*). The thresholds, which were calculated as the cholesterol concentration at which the fitted curves rise to between 2.5 and 25% of their maximal value, show PFO binding to DOPC liposomes at 26.5–31.5 mol % cholesterol and binding to POPC liposomes at 40.4–45.0 mol % cholesterol.

To compare this experimental binding data to the simulations, we identified three potential structural measures of cholesterol accessibility in our simulations: cholesterol depth within the bilayer, cholesterol SASA, and cholesterol-water hydrogen bonding. All of these measures were expected to be strongly related to cholesterol availability for binding. We chose cholesterol depth as our primary measurement of cholesterol accessibility because it provided the most consistent data, though all metrics were highly correlated. The other metrics are shown in the Supporting Material (see Fig. S2). Changes in mean cholesterol depth in the bilayer are shown in Fig. 2 *B*.

In both POPC and DOPC membranes, mean cholesterol depth is constant at low concentrations: in DOPC membranes, we see no statistically significant changes from 5 to 18 mol %, whereas depth in POPC membranes

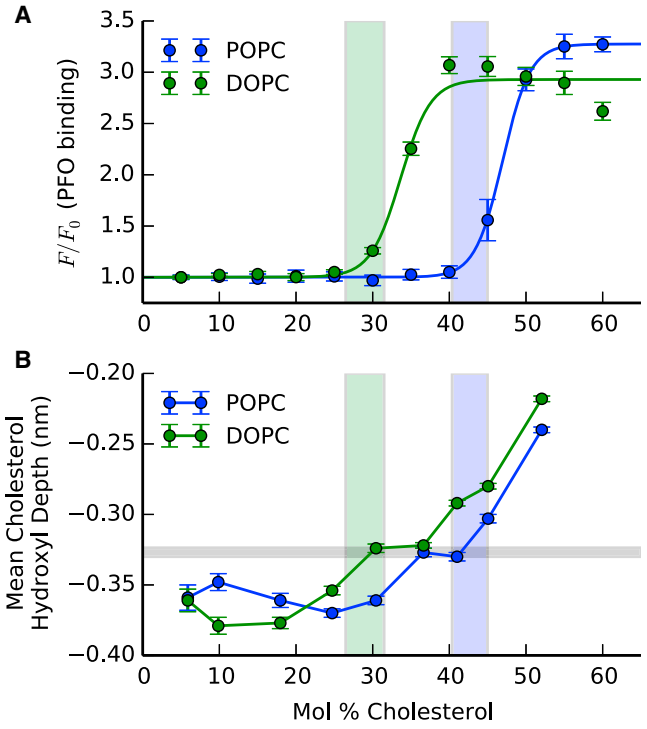

FIGURE 2 Cholesterol activation as measured in experimental and simulated membrane systems. (*A*) Binding of perfringolysin O to liposomes composed of POPC (*blue*) or DOPC (*green*) membranes of varying cholesterol concentrations. Error bars are derived from four replica experiments. (*Solid lines*) Sigmoidal fits to the binding data. (*Shaded regions*) Region of 2.5–25% of maximal binding, as estimated from the fit. (*B*) Mean cholesterol hydroxyl depth for cholesterol in simulated POPC (*blue*) or DOPC (*green*) membranes of varying cholesterol concentrations. Error bars show standard deviations of the mean. POPC (*shaded blue*) and DOPC (*green*) regions are calculated from the experimental data shown in panel *A*. (*Gray region*) Estimated mean depth of 0.33 nm at which PFO binding occurs for both lipid species.

is unchanging up to 30 mol %. Above these composition-dependent thresholds, we see a significant and consistent rise in mean depth, with depth increasing roughly linearly with concentration above the threshold. These increases past the saturation thresholds are indicative of cholesterol activation as cholesterol shifts closer to the bilayer/water interface.

Comparison of the experimentally determined PFO binding thresholds with the simulation data reveal that PFO binding is initially observed in both POPC and DOPC membranes at concentrations ~10 mol % above the saturation threshold for cholesterol depth. In POPC membranes, this saturation threshold is 30 mol %, with PFO binding observed at 40 mol %, whereas in DOPC membranes the saturation threshold is lower, at 18 mol %, with PFO binding observed at 27 mol %. Moreover, mean cholesterol depth curves for both POPC and DOPC membranes cross the PFO binding thresholds at a common value of −0.33 nm. Together, this suggests that binding of PFO is dependent on the presence of particularly exposed cholesterol molecules and that the degree of exposure required for binding is independent of phospholipid composition, with differences between POPC and DOPC membranes caused by a lower saturation threshold for cholesterol activity in DOPC membranes.

Because cholesterol depth is defined by the relative position of cholesterol molecules and the water interface, the large increases in depth we observe above saturation thresholds can be caused by movements in either interface or cholesterol positions. We thus calculated the cholesterol and interface positions separately to identify the source of the observed increase in cholesterol accessibility (Fig. 3 *A*). We find that in the low-cholesterol condensation regime, the interface position shifts outward as the membrane thickens, but cholesterol positions shift outward concurrently, resulting in no net change in their relative positions. Because the membrane structure is altered at higher cholesterol concentrations, the water interface moves inward while the cholesterol position remains close to its maximal value, causing partial cholesterol exposure with increased water penetration of the bilayer. The sources of the increased accessibility of cholesterol in DOPC versus POPC membranes can also be identified from this data. At lower concentrations, increased accessibility is caused by a smaller

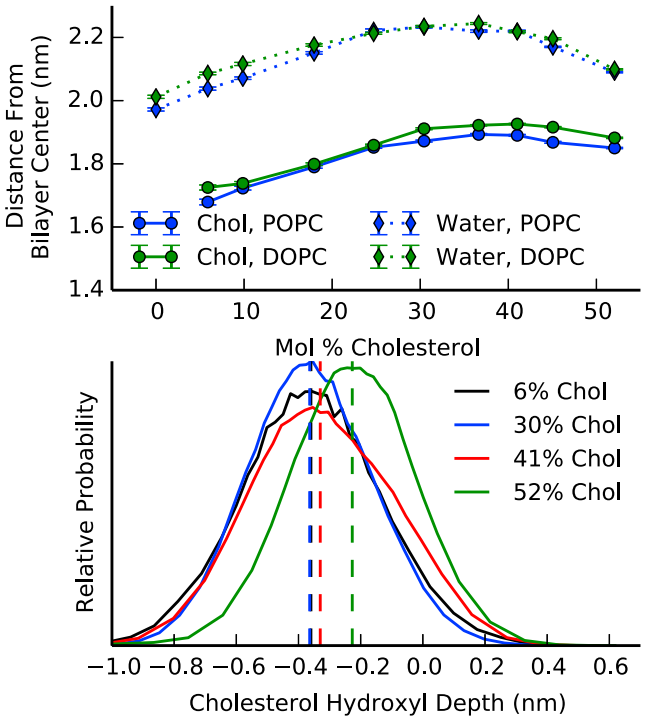

FIGURE 3 (*A*) Mean positions of cholesterol hydroxyl oxygens (*solid*) and the bilayer/water interface (*dotted*), measured relative to the bilayer center, in POPC (*blue*) or DOPC (*green*) membranes at varying cholesterol concentrations. Error bars show standard deviations of the mean. (*B*) Distributions of cholesterol depth in POPC bilayers with 6 (*black*), 30 (*blue*), 41 (*red*), and 52 (*green*) mol % cholesterol. (*Dashed vertical lines*) Medians of each distribution.

outward movement of the water interface, presumably due to the more disordered unsaturated acyl chains of DOPC being less able to pack efficiently into a condensed membrane. At higher concentrations, we see the water interface behave similarly between both membranes, but cholesterol in DOPC membranes stabilizes significantly closer to the water interface than in POPC membranes, perhaps due to lower affinity of cholesterol for unsaturated acyl chains.

Changes in mean cholesterol accessibility could be driven by either shifts in an equilibrium between distinct states of unavailable, deeper cholesterol and available, more exposed cholesterol, or instead by general increases in the accessibility of all membrane cholesterols. To compare these models, we examined the normalized distributions of cholesterol depth for four representative POPC/cholesterol bilayers: 6, 30, 41, and 52 mol % cholesterol (Fig. 3 *B*). Similar results were obtained for DOPC bilayers (see Fig. S3). From 6 to 30%, the distributions show no significant change as measured through Kolmogorov-Smirnov statistical tests. At higher concentrations, the entire distribution shifts to increased exposure, with the median of the 52% distribution shifted toward the bilayer-water interface by 0.13 nm. The distributions remain unimodal, with no clear separation between distinct active and inactive subpopulations of cholesterol. Thus, the observed increase in cholesterol accessibility is not specific to a subset of available cholesterol molecules, but instead cholesterol in general becomes more available at high concentrations as the bilayer thins and partially exposes cholesterol.

LOCAL VERSUS GLOBAL EFFECTS

We observe significant changes in measures of lipid condensation and cholesterol accessibility with increased cholesterol concentration. To identify whether these changes occur uniformly in all lipids or are restricted to lipids in a particular local environment, we calculated neighbor-neighbor interactions between phospholipid and cholesterol in each leaflet of the membrane. Each lipid has on average six neighbors, but the identity of these neighbors will vary with concentration; as the concentration of cholesterol increases, the number of cholesterol neighbors will increase, while being somewhat randomly distributed. This allows us to separate lipids into various categories depending on the numbers and types of their neighbors.

Phospholipids were divided into two groups: those with one or more cholesterol neighbors and those with no neighboring cholesterol. Percentages of phospholipids in these two categories are shown in Fig. 4 *A*. Behavior is identical in both POPC and DOPC bilayers; the percentage of phospholipids near cholesterol rises from 0% when no cholesterol is present to >90% at 25 mol % cholesterol. Above 25 mol % cholesterol, nearly all phospholipids neighbor at least one cholesterol molecule. This concentration range is similar to the range in which membrane condensation is observed, suggesting that membrane condensation is driven by extending the local condensing effects of cholesterol to a wider fraction of phospholipids. This was tested by comparing the mean phospholipid-tail order of lipids near or distant from cholesterol, as shown in Fig. 4 *B*. At all concentrations where significant fractions of near and distant phospholipids are present, phospholipids nearby cholesterol show, on average, significantly higher tail-order than more distant lipids. This suggests that local ordering of phospholipids is directly induced by the presence of nearby cholesterol molecules, and that this increase in phospholipid order saturates when all phospholipids in the membrane are sufficiently close to cholesterol to be condensed.

To examine whether changes in cholesterol accessibility are similarly dependent on the local environment, we similarly divided cholesterol into two groups based on their number of phospholipid neighbors. We chose an arbitrary

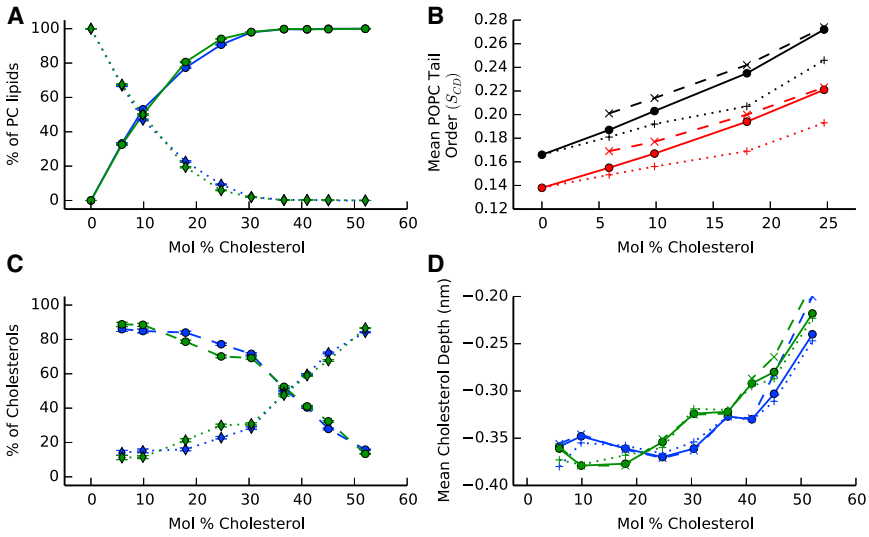

FIGURE 4 (*A*) Percentage of POPC (*blue*) or DOPC (*green*) phospholipids that are neighbors of (*solid*) or distant from (*dotted*) cholesterol molecules in each bilayer leaflet. (*B*) Mean tail-order parameters for the sn-1 palmitoyl (*black*) and sn-2 oleoyl (*red*) chains of POPC, shown as the mean over all phospholipids (*solid*) or only those phospholipids that are neighbors of (*dashed*) or distant from (*dotted*) cholesterol molecules in each bilayer leaflet. (*C*) Percentage of cholesterol molecules in POPC (*blue*) or DOPC (*green*) membranes that have >4 (*dashed*), or ≤4 (*dotted*) phospholipid neighbors. (*D*) Depth of cholesterol hydroxyl oxygens in POPC (*blue*) or DOPC (*green*) membranes, shown as the mean over all cholesterols (*solid*), over only cholesterols with ≤4 PC neighbors (*dotted*), or over only cholesterols with >4 PC neighbors (*dashed*).

division line to separate cholesterols: those with four or fewer PC neighbors composed one group and those with more than four, another. Although this particular division is arbitrary, the results are not strongly dependent on the choice of boundary, with similar results for division lines from two-to-six PC neighbors. Fig. 4 *C* shows the relative population of cholesterols with high or low numbers of PC neighbors. We find that at low concentrations, more cholesterols are found in the high neighbor population and that this preference shifts as the cholesterol concentration rises. In Fig. 2 *D*, we show mean cholesterol depth values for all cholesterols; for those only with high numbers of PC neighbors; and for those only with low numbers of PC neighbors. We find no statistically significant differences in mean depth between cholesterols with low and high numbers of PC neighbors, indicating that local environment is not important for determining cholesterol accessibility.

DISCUSSION

In this study, we examine the molecular basis of cholesterol activation, a key step in the rapid, nongenomic physiological response to excess cholesterol. In agreement with previous experimental and simulation reports, we find that at lower cholesterol concentrations, cholesterol induces a well-characterized condensation of phosphatidylcholine membranes, as seen by decreased phospholipid exposure to solvent, membrane thickening, and ordering of the lipid tails (6,7,36–40). This condensing effect is driven by the local ordering of phospholipids induced by neighboring cholesterol molecules and saturates at 25–30 mol % cholesterol, at which point nearly all phospholipids are sufficiently close to cholesterol to be condensed. Above this saturation point, we find a partial reversal of some of these cholesterol-driven changes in membrane organization. Whereas phospholipid SASA increases and membrane thickness decreases, indicating decreased membrane condensation, phospholipid-tail order continues to increase and only drops slightly at very high cholesterol concentrations. The membrane thinning at high concentrations is driven not by disorder of the lipid tails but instead by increased phospholipid interdigitation, which allows tighter packing in the bilayer interior. This indicates that the changes occurring at high cholesterol concentrations are not a simple reversal of the condensation observed at low concentrations, but instead reflect a believed new and different alteration of general membrane structure.

In addition to these measures of general membrane structure, we have also directly measured changes in individual cholesterol structure and orientation that we believe correspond to cholesterol accessibility. Activation of cholesterol triggers sterol homeostatic responses by increasing availability of cholesterol to extramembrane acceptors (e.g., for transfer between membranes) or for interaction with membrane proteins (e.g., sterol-sensing or sterol-binding proteins) (42).

Three lines of evidence suggest that the key step in cholesterol activation is the movement of cholesterol into orientations more highly exposed to solvent:

1. An increase in availability to external binding molecules like PFO for cholesterols in more-exposed orientations is intuitively plausible; we would expect cholesterol that is more exposed to solvent to also be more exposed to binding partners present in the solvent.
2. Previous simulations examining the membrane behavior of side-chain oxysterols—potent effectors of cholesterol activation—demonstrated that in mixed cholesterol-oxysterol membranes, oxysterol-induced membrane disordering was accompanied by membrane thinning and increased exposure of cholesterol (23).
3. In this study we have shown that increases in mean cholesterol depth, a measure of cholesterol exposure, is associated with PFO binding in both POPC and DOPC membranes, and that cholesterol in both membranes begins to be available for binding only once the mean depth reaches a threshold of roughly −0.33 nm.

The original cholesterol activation hypothesis first proposed by Lange, Steck, and co-workers (15–18) posited that cholesterol activation was driven by the saturation of cholesterol binding sites in the membrane, leading to excess cholesterol adopting unbound, more accessible orientations. This model implies that:

1. Cholesterol should exist in two distinct pools, with unavailable cholesterol retaining strong interactions with phospholipids and available cholesterol weaker ones; and
2. Population of the available pool should grow as the cholesterol concentration rises above the threshold concentration.

The formation of and saturation of cholesterol-phospholipid complexes is supported by simulation data showing strong hydrogen-bonding interactions between cholesterol and phospholipids (23,25,36–40) as well as monolayer experiments consistent with theoretical models of complex formation (43–46). This saturation model is consistent with our results showing that membrane condensation of phospholipids by cholesterol is local with respect to the direct neighbors of each cholesterol molecule.

These cholesterol-phospholipid interactions, however, are not directly responsible for the activation of cholesterol. We do not find cholesterol partitioned into distinct available and unavailable pools. Instead, we find that distributions of cholesterol depth remain unimodal at all concentrations. The increase in mean cholesterol accessibility at high concentrations is caused by a shift in the distribution as a whole rather than a transfer from low to high accessibility pools. Further, we find no dependence of cholesterol accessibility

on its local environment; cholesterols with fewer neighboring phospholipids show no higher accessibility than those with more. Cholesterol activation appears to instead be driven by global changes in membrane-cholesterol interactions, rather than disruption or saturation of local phospholipid interactions causing partial cholesterol release. Examination of cholesterol and interface positions shows that reduced cholesterol depth (i.e., increased cholesterol accessibility) at high cholesterol concentrations is largely due to inward movement of the bilayer/water interface rather than the outward movement of cholesterol, and thus is directly related to membrane thinning and other changes in global membrane behavior. The lowered concentration required for cholesterol activation in DOPC versus POPC membranes is likely caused by stabilization of cholesterol farther from the membrane interior, which may be linked to a decreased affinity of cholesterol for the more disordered acyl chains of DOPC. We expect that similar measurements done on membranes composed of other lipids will show the same relationship between lowered cholesterol activation thresholds and decreased cholesterol-acyl chain affinity, as supported by PFO binding data showing lower activation thresholds in membranes of branched lipids (19).

The simulations and the PFO liposome experiments provide orthogonal yet complementary approaches to assess cholesterol behavior in membranes. The relationship between the continuous model of cholesterol activity and the experimental measurements of cholesterol binding is presented in Fig. 5. We propose that at low concentrations, in the condensation phase, mean cholesterol accessibility is low and constant. Above some saturation threshold C_{sat}, dependent on the transition between a condensing and a relaxing membrane and the affinity of cholesterol for its phospholipid neighbors, mean cholesterol accessibility begins increasing linearly with concentration (Fig. 5 *A*). Because cholesterol accessibility is continuous rather than discrete, at each concentration there is a range of cholesterols present of varying accessibility. Some fraction of the cholesterol at each concentration will have accessibility above the relatively high threshold $A_{binding}$ required to be available for binding to PFO or other external molecules (Fig. 5 *B*). The concentration of available cholesterol, with accessibility greater than this threshold, will thus increase nonlinearly with total cholesterol concentration, both because the size of the total pool increases and because the fraction of the pool above the threshold $A_{binding}$ increases (Fig. 5 *C*). A binding molecule that binds only to available cholesterol will then show a sharp transition between unbound and bound states around the threshold concentration $C_{binding}$, where significant amounts of available cholesterol appear in the membrane (Fig. 5 *D*).

We propose a revised biophysical model for the underlying structural basis and causes of cholesterol activation (Fig. 6). As the membrane cholesterol concentration rises, cholesterol induces local ordering of lipid acyl chains. These ordered acyl chains are more extended, causing the membrane to condense laterally and thicken to accommodate the extended chains. However, because cholesterol is shorter than the extended phospholipid acyl chains but retained near the interface due to its amphipathic nature, unfavorable free space in the bilayer interior begins to form as the phospholipids are pushed apart laterally by increasing concentrations of cholesterol. At a defined threshold concentration that is dependent on the membrane lipid composition, the membrane leaflets interdigitate to resolve the unfavorable free space, thinning the bilayer and spreading phospholipids laterally, consequently allowing greater water penetration into the bilayer interface. This increased water penetration and inward movement of the phospholipids exposes the cholesterol, which is observed experimentally as activation. Interestingly, similar activation thresholds can be observed in monolayer studies (44), suggesting that leaflet interdigitation is secondary to membrane thinning, which we hypothesize would proceed primarily through lipid-chain disordering in monolayer systems.

This model may also explain the mechanism through which structurally diverse amphiphiles are known to activate cholesterol (24). By selectively incorporating in the headgroup region of the bilayer, amphiphiles would similarly cause an increase in interior bilayer free space, driving membrane thinning and cholesterol activation in a similar

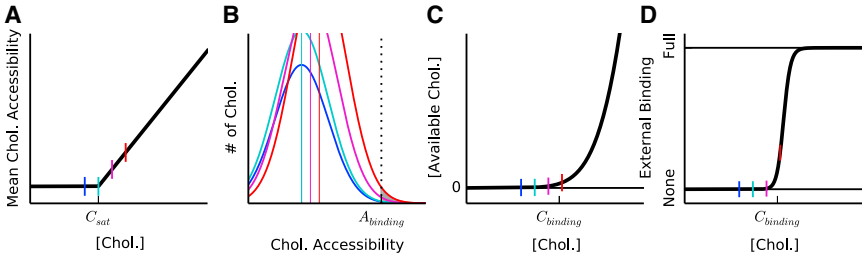

FIGURE 5 The proposed relation between underlying changes in cholesterol accessibility and experimentally measured binding to available cholesterol. (Four concentrations of cholesterol are marked in *blue*, *cyan*, *magenta*, and *red* in all four panels for comparison.) (*A*) Mean cholesterol accessibility is modeled as constant below a saturation threshold C_{sat} and increasing linearly above it. (*B*) The number of cholesterols of each accessibility at any particular concentration (*thick lines*) are modeled as normal distributions centered on the mean value (*thin lines*) and with a common variance. Those cholesterols above some high threshold $A_{binding}$ are presumed to be available for binding to external acceptors. (*C*) The concentration of available cholesterol changes nonlinearly with total cholesterol concentration, with significant amounts of available cholesterol occurring only above the binding threshold $C_{binding}$. (*D*) Binding of an external acceptor is dependent only on the concentration of available cholesterol, and thus occurs only above $C_{binding}$ before saturating once all acceptors have bound cholesterol.

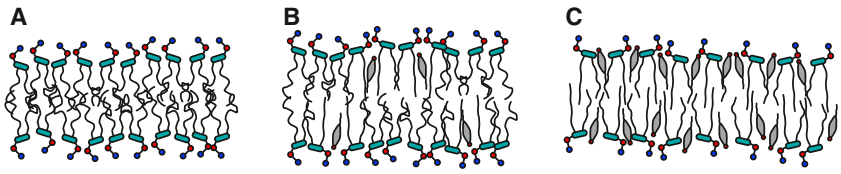

FIGURE 6 The proposed model of cholesterol activation. (*A*) With no cholesterol present, phospholipids pack loosely with their tails in relatively disordered states. (*B*) As cholesterol is added to the membrane, it locally orders neighboring phospholipids, causing the bilayer to thicken and condense. (*C*) At very high cholesterol concentrations, length mismatch between cholesterol and phospholipids drives interdigitation of the acyl chains, resulting in membrane thinning and cholesterol exposure to solvent.

manner. In our previous study of oxysterol effects on cholesterol activation, we found that significant membrane thinning caused by oxysterols was associated with cholesterol activation (23). The low concentrations of oxysterols found in physiological systems are believed to signal in cholesterol regulation pathways partially through their effects on membrane structure (23,47). This model for cholesterol activation as a byproduct of general membrane thinning has immediate relevance for study of oxysterol-induced cholesterol activation, in particular examining the composition- and concentration-dependence of oxysterol effects in model membrane and physiological systems.

SUPPORTING MATERIAL

Three figures and references (48, 49) are available at http://www.biophysj.org/biophysj/supplemental/S0006-3495(13)00989-2.

The authors thank Katherine Henzler-Wildman for numerous helpful discussions, Ted Steck and Yvonne Lange for insightful comments on the manuscript, and Alejandro Heuck for generously providing the PFO expression construct.

This work was supported by the National Institutes of Health through grant No. R01 HL067773. B.N.O. was supported by the Institutional Cardiovascular Biology Training Grant, grant No. T32HL007275. A.A.G. was supported by the National Institutes of Health (NIH) through grant No. F30 HL97563. Computational resources were provided by the Texas Advanced Computing Center through Teragrid grants No. TG-MCB060053 and TG-MCA08X003 as well as the National Biomedical Computation Resource through grant No. NIH P41 RR0860516. This work used the Extreme Science and Engineering Discovery Environment (XSEDE), which is supported by the National Science Foundation through grant No. OCI-1053575.

REFERENCES

1. Liscum, L., and N. J. Munn. 1999. Intracellular cholesterol transport. *Biochim. Biophys. Acta*. 1438:19–37.
2. Ohvo-Rekilä, H., B. Ramstedt, …, J. P. Slotte. 2002. Cholesterol interactions with phospholipids in membranes. *Prog. Lipid Res*. 41:66–97.
3. van Meer, G., D. R. Voelker, and G. W. Feigenson. 2008. Membrane lipids: where they are and how they behave. *Nat. Rev. Mol. Cell Biol*. 9:112–124.
4. Nezil, F. A., and M. Bloom. 1992. Combined influence of cholesterol and synthetic amphiphilic peptides upon bilayer thickness in model membranes. *Biophys. J*. 61:1176–1183.
5. Purdy, P. H., M. H. Fox, and J. K. Graham. 2005. The fluidity of Chinese hamster ovary cell and bull sperm membranes after cholesterol addition. *Cryobiology*. 51:102–112.
6. Hung, W.-C., M.-T. Lee, …, H. W. Huang. 2007. The condensing effect of cholesterol in lipid bilayers. *Biophys. J*. 92:3960–3967.
7. Warschawski, D. E., and P. F. Devaux. 2005. Order parameters of unsaturated phospholipids in membranes and the effect of cholesterol: a ^{1}H-^{13}C solid-state NMR study at natural abundance. *Eur. Biophys. J*. 34:987–996.
8. Martinez, G. V., E. M. Dykstra, …, M. F. Brown. 2002. NMR elastometry of fluid membranes in the mesoscopic regime. *Phys. Rev. E Stat. Nonlin. Soft Matter Phys*. 66:50902.
9. Endress, E., H. Heller, …, T. M. Bayerl. 2002. Anisotropic motion and molecular dynamics of cholesterol, lanosterol, and ergosterol in lecithin bilayers studied by quasi-elastic neutron scattering. *Biochemistry*. 41:13078–13086.
10. Brown, M. S., and J. L. Goldstein. 1997. The SREBP pathway: regulation of cholesterol metabolism by proteolysis of a membrane-bound transcription factor. *Cell*. 89:331–340.
11. Horton, J. D., J. L. Goldstein, and M. S. Brown. 2002. SREBPs: activators of the complete program of cholesterol and fatty acid synthesis in the liver. *J. Clin. Invest*. 109:1125–1131.
12. Goldstein, J. L., and M. S. Brown. 1990. Regulation of the mevalonate pathway. *Nature*. 343:425–430.
13. Gil, G., J. R. Faust, …, M. S. Brown. 1985. Membrane-bound domain of HMG CoA reductase is required for sterol-enhanced degradation of the enzyme. *Cell*. 41:249–258.
14. Cheng, D., C. C. Chang, …, T. Y. Chang. 1995. Activation of acyl-coenzyme A:cholesterol acyltransferase by cholesterol or by oxysterol in a cell-free system. *J. Biol. Chem*. 270:685–695.
15. Lange, Y., J. Ye, and T. L. Steck. 2004. How cholesterol homeostasis is regulated by plasma membrane cholesterol in excess of phospholipids. *Proc. Natl. Acad. Sci. USA*. 101:11664–11667.
16. Lange, Y., T. L. Steck, …, D. Ory. 2009. Regulation of fibroblast mitochondrial 27-hydroxycholesterol production by active plasma membrane cholesterol. *J. Lipid Res*. 50:1881–1888.
17. Lange, Y., J. Ye, …, T. L. Steck. 1999. Regulation of endoplasmic reticulum cholesterol by plasma membrane cholesterol. *J. Lipid Res*. 40:2264–2270.
18. Steck, T. L., and Y. Lange. 2010. Cell cholesterol homeostasis: mediation by active cholesterol. *Trends Cell Biol*. 20:680–687.
19. Sokolov, A., and A. Radhakrishnan. 2010. Accessibility of cholesterol in endoplasmic reticulum membranes and activation of SREBP-2 switch abruptly at a common cholesterol threshold. *J. Biol. Chem*. 285:29480–29490.
20. Flanagan, J. J., R. K. Tweten, …, A. P. Heuck. 2009. Cholesterol exposure at the membrane surface is necessary and sufficient to trigger perfringolysin O binding. *Biochemistry*. 48:3977–3987.
21. Ali, M. R., K. H. Cheng, and J. Huang. 2007. Assess the nature of cholesterol-lipid interactions through the chemical potential of cholesterol in phosphatidylcholine bilayers. *Proc. Natl. Acad. Sci. USA*. 104:5372–5377.
22. Brown, M. S., S. E. Dana, and J. L. Goldstein. 1975. Cholesterol ester formation in cultured human fibroblasts. Stimulation by oxygenated sterols. *J. Biol. Chem*. 250:4025–4027.

23. Olsen, B. N., P. H. Schlesinger, …, N. A. Baker. 2011. 25-Hydroxycholesterol increases the availability of cholesterol in phospholipid membranes. *Biophys. J.* 100:948–956.

24. Lange, Y., J. Ye, …, T. L. Steck. 2009. Activation of membrane cholesterol by 63 amphipaths. *Biochemistry.* 48:8505–8515.

25. Olsen, B. N., P. H. Schlesinger, and N. A. Baker. 2009. Perturbations of membrane structure by cholesterol and cholesterol derivatives are determined by sterol orientation. *J. Am. Chem. Soc.* 131:4854–4865.

26. Berger, O., O. Edholm, and F. Jähnig. 1997. Molecular dynamics simulations of a fluid bilayer of dipalmitoylphosphatidylcholine at full hydration, constant pressure, and constant temperature. *Biophys. J.* 72:2002–2013.

27. Kandt, C., W. L. Ash, and D. P. Tieleman. 2007. Setting up and running molecular dynamics simulations of membrane proteins. *Methods.* 41:475–488.

28. Berendsen, H. J. C., J. R. Grigera, and T. P. Straatsma. 1987. The missing term in effective pair potentials. *J. Phys. Chem.* 91:6269–6271.

29. Berendsen, H. J. C., D. van der Spoel, and R. van Drunen. 1995. GROMACS: a message-passing parallel molecular dynamics implementation. *Comput. Phys. Commun.* 91:43–56.

30. Lindahl, E., B. Hess, and D. van Der Spoel. 2001. GROMACS 3.0: a package for molecular simulation and trajectory analysis. *J. Mol. Model.* 7:306–317.

31. Baker, N. A., D. Sept, …, J. A. McCammon. 2001. Electrostatics of nanosystems: application to microtubules and the ribosome. *Proc. Natl. Acad. Sci. USA.* 98:10037–10041.

32. Egberts, E., and H. J. C. Berendsen. 1988. Molecular dynamics simulation of a smectic liquid crystal with atomic detail. *J. Chem. Phys.* 89:3718.

33. Song, Y., V. Guallar, and N. A. Baker. 2005. Molecular dynamics simulations of salicylate effects on the micro- and mesoscopic properties of a dipalmitoylphosphatidylcholine bilayer. *Biochemistry.* 44:13425–13438.

34. Patra, M., E. Salonen, …, M. Karttunen. 2006. Under the influence of alcohol: the effect of ethanol and methanol on lipid bilayers. *Biophys. J.* 90:1121–1135.

35. Pan, H., O. Ivashyna, …, S. A. Wickline. 2011. Post-formulation peptide drug loading of nanostructures for metered control of NF-κB signaling. *Biomaterials.* 32:231–238.

36. Chiu, S. W., E. Jakobsson, …, H. L. Scott. 2002. Cholesterol-induced modifications in lipid bilayers: a simulation study. *Biophys. J.* 83: 1842–1853.

37. Alwarawrah, M., J. Dai, and J. Huang. 2010. A molecular view of the cholesterol condensing effect in DOPC lipid bilayers. *J. Phys. Chem. B.* 114:7516–7523.

38. Róg, T., and M. Pasenkiewicz-Gierula. 2006. Cholesterol effects on a mixed-chain phosphatidylcholine bilayer: a molecular dynamics simulation study. *Biochimie.* 88:449–460.

39. Pandit, S. A., D. Bostick, and M. L. Berkowitz. 2004. Complexation of phosphatidylcholine lipids with cholesterol. *Biophys. J.* 86:1345–1356.

40. Pandit, S. A., S. W. Chiu, …, H. L. Scott. 2008. Cholesterol packing around lipids with saturated and unsaturated chains: a simulation study. *Langmuir.* 24:6858–6865.

41. Heuck, A. P., E. M. Hotze, …, A. E. Johnson. 2000. Mechanism of membrane insertion of a multimeric β-barrel protein: perfringolysin O creates a pore using ordered and coupled conformational changes. *Mol. Cell.* 6:1233–1242.

42. Bielska, A. A., P. Schlesinger, …, D. S. Ory. 2012. Oxysterols as non-genomic regulators of cholesterol homeostasis. *Trends Endocrinol. Metab.* 23:99–106.

43. Radhakrishnan, A., and H. McConnell. 2005. Condensed complexes in vesicles containing cholesterol and phospholipids. *Proc. Natl. Acad. Sci. USA.* 102:12662–12666.

44. Radhakrishnan, A., and H. M. McConnell. 2000. Chemical activity of cholesterol in membranes. *Biochemistry.* 39:8119–8124.

45. Radhakrishnan, A., and H. M. McConnell. 1999. Condensed complexes of cholesterol and phospholipids. *Biophys. J.* 77:1507–1517.

46. McConnell, H. 2003. Condensed complexes of cholesterol and phospholipids. *Biochim. Biophys. Acta. Biomembr.* 1610:159–173.

47. Gale, S. E., E. J. Westover, …, D. S. Ory. 2009. Side chain oxygenated cholesterol regulates cellular cholesterol homeostasis through direct sterol-membrane interactions. *J. Biol. Chem.* 284:1755–1764.

48. Greenwood, A. I., S. Tristram-Nagle, and J. F. Nagle. 2006. Partial molecular volumes of lipids and cholesterol. *Chem. Phys. Lipids.* 143:1–10.

49. Hofsäss, C., E. Lindahl, and O. Edholm. 2003. Molecular dynamics simulations of phospholipid bilayers with cholesterol. *Biophys. J.* 84:2192–2206.